

**A model for aromatic
SOA formation by
multiphase reactions**

Y. Im et al.

Simulation of aromatic SOA formation using the lumping model integrated with explicit gas-phase kinetic mechanisms and aerosol-phase reactions

Y. Im, M. Jang, and R. L. Beardsley

Department of Environmental Engineering Sciences, University of Florida, P.O. Box 116450, Gainesville, FL 32611, USA

Received: 18 December 2012 – Accepted: 14 February 2013 – Published: 6 March 2013

Correspondence to: M. Jang (mjang@ufl.edu)

Published by Copernicus Publications on behalf of the European Geosciences Union.

Title Page

Abstract

Introduction

Conclusions

References

Tables

Figures



Back

Close

Full Screen / Esc

Printer-friendly Version

Interactive Discussion



Abstract

The Unified Partitioning-Aerosol phase Reaction (UNIPAR) model has been developed to predict the secondary organic aerosol (SOA) formation through multiphase reactions. An explicit gas-kinetic model was employed to express gas-phase oxidation of aromatic hydrocarbons. Gas-phase products are grouped based on volatility (6 levels) and reactivity (5 levels) and used to construct the stoichiometric coefficients ($\alpha_{i,j}$) matrix, the set of parameters used to describe the concentrations of organic compounds in multiphase. Weighting of the $\alpha_{i,j}$ matrix as a function of NO_x improved the evaluation of NO_x effects on SOA. The total amount of organic matter (OM_T) is predicted by two modules in the UNIPAR model: OM_P by a partitioning process and OM_{AR} by aerosol-phase reactions. OM_P is estimated using the SOA partitioning model that has been used in a regional air quality model (CMAQ 5.0.1). OM_{AR} predicts multiphase reactions of organic compounds, such as oligomerization, acid-catalyzed reactions, and organosulfate (OS) formation. The model was evaluated with the SOA data produced from the photooxidation of toluene and 1,3,5-trimethylbenzene using an outdoor reactor (UF-APHOR chamber). The model reasonably simulates SOA formation under various aerosol acidities, NO_x concentrations, humidities and temperatures. Furthermore, the OS fraction in the SOA predicted by the model was in good agreement with the experimentally measured OS fraction.

1 Introduction

Organic aerosols have attracted the interest of many researchers because of the significant role they play in climate forcing (IPCC, 2001), human health (Schwartz et al., 1996), and visibility (Bäumer et al., 2008). The oxidation of reactive volatile organic hydrocarbons (VOCs) produces semivolatile multifunctional products that can form secondary organic aerosols (SOA) through either gas-particle partitioning or aerosol-phase reactions. Although SOA make up a major fraction of atmospheric aerosol, the

ACPD

13, 5843–5870, 2013

A model for aromatic SOA formation by multiphase reactions

Y. Im et al.

Title Page

Abstract

Introduction

Conclusions

References

Tables

Figures

◀

▶

◀

▶

Back

Close

Full Screen / Esc

Printer-friendly Version

Interactive Discussion



development of a model to predict the formation of SOA remains difficult, due to the complexity of formation mechanisms in both the gas and aerosol phases as well as the diversity of compounds (a large fraction of which remain unidentified).

Previously, the complex task of predicting SOA formation was facilitated by the gas-particle partitioning model, which uses a few semivolatile surrogate products (Odum et al., 1996) derived from the photooxidation of VOCs. These products are semiempirically fit to chamber produced SOA yields using mass-based stoichiometric parameters and equilibrium partitioning coefficients. Although this model advanced the prediction of SOA formation, its simple parameterization is limited to a wide range of volatility of atmospheric organic products and multi-generational oxidation processes (particle aging) in both gas and particle phases (Donahue et al., 2006). It also does not account for aerosol-phase chemistry, which can significantly increase SOA mass, forming nonvolatile high molecular weight (MW) compounds. In particular, many studies have recently reported that SOA formation is accelerated by acid-catalyzed reactions (e.g. hydration, polymerization, formation of hemiacetal/acetal/trioxane, aldol condensation, and cationic rearrangement) (Jang and Kamens, 2001; Garland et al., 2006) in the presence of inorganic aerosol for both the oxidation products of biogenic (Czoschke et al., 2003; Iinuma et al., 2004; Kleindienst et al., 2006; Surratt et al., 2007) and aromatic hydrocarbons (Cao and Jang, 2007, 2010). Furthermore, it also has been found that a new class of products, organosulfate (OS), can be formed through the aerosol-phase reaction of organic species either with sulfate, bisulfate (Betters et al., 1987; Liggio et al., 2005) or their radicals (Galloway et al., 2009; Olson et al., 2011; Darer et al., 2011).

There have been many efforts to integrate recent discoveries in aerosol phase chemistry into SOA models. For example, Donahue et al. (2006) have attempted to add the particle-aging process to a SOA model using the volatility basis set (VBS) approach. In their model, the volatility distribution of products was represented using a group of volatility bins, and the multigenerational oxidations of semivolatile organic compounds (SVOCs) was illustrated by remapping the products in the volatility bins. Cappa and

A model for aromatic SOA formation by multiphase reactions

Y. Im et al.

Title Page

Abstract

Introduction

Conclusions

References

Tables

Figures

◀

▶

◀

▶

Back

Close

Full Screen / Esc

Printer-friendly Version

Interactive Discussion



A model for aromatic SOA formation by multiphase reactions

Y. Im et al.

Title Page

Abstract

Introduction

Conclusions

References

Tables

Figures

◀

▶

◀

▶

Back

Close

Full Screen / Esc

Printer-friendly Version

Interactive Discussion

Willson (2012) have recently simulated SOA mass and bulk aerosol O : C atomic ratios employing tunable parameters to describe the kinetic evolution of SOA mass due to precursor VOC oxidation and further oxidation of gas phase products. Some models have integrated the explicit gas-phase kinetic mechanisms of oxidation of VOCs with gas-particle partitioning. For example, Kamens et al. (1999) predicted the SOA formation through the kinetically represented gas-particle partitioning of SVOCs by the ratio of rate constants of condensation to evaporation in the gas-kinetic mechanism. However, these models are limited in their ability to represent the details of complex aerosol-phase chemistry including the interaction between organic and inorganic compounds. The latest version of the regional air quality model (CMAQ 5.0.1) has attempted to incorporate aerosol chemistries by including simplified oligomerization reactions and acid-catalyzed uptake of isoprene SOA. Although such efforts have been devoted to improving the understanding of aerosol phase reactions, current air quality models still significantly underestimate ambient organic matter (OM) measured in the field (Simpson et al., 2007; Kleinman et al., 2008).

Jang et al. (2006) have recently developed a SOA model that includes acid-catalyzed reactions of organic compounds in the presence of inorganic seed aerosol. In this model, the SVOCs predicted by explicit gas-phase kinetic mechanisms are classified using 20 lumping species based on the volatility and reactivity for aerosol-phase reactions. The SOA mass from the aerosol-phase reaction is predicted using the aerosol phase rate constants, which incorporate acidity and molecular structures. This approach was applied to SOA formation from the ozonolysis of α -pinene (Jang et al., 2006) and oxidation of toluene with NO_x (Cao and Jang, 2010). While this model advanced the prediction of SOA by considering the effect of acidity on SOA formation, some limitations remained. For example, the gas-phase aging of organic compounds and organosulfate formation were not considered. In terms of expression of aerosol chemistry, this model was also limited in handling dynamically changing aerosol acidity (e.g. ammonia titration of acidic aerosol and acidity change by OS formation).

A model for aromatic SOA formation by multiphase reactions

Y. Im et al.

Title Page

Abstract

Introduction

Conclusions

References

Tables

Figures

◀

▶

◀

▶

Back

Close

Full Screen / Esc

Printer-friendly Version

Interactive Discussion



In the present study, the SOA model developed using indoor chamber studies by Cao and Jang et al. (2010) was advanced in order to include multiphase reactions of organic compounds and recently discovered aerosol-phase chemistry such as the formation of OS using outdoor chamber data. The Unified Partitioning-Aerosol phase Reaction (UNIPAR) model of this study has revised the previous model to allow for simulation of SOA formation under dynamically changing atmospheric conditions (NO_x , temperature, humidity, sunlight and particle acidity). In the UNIPAR model, oligomerization is described in both organic and inorganic aerosol phases, and the formation of OS is predicted in various experimental conditions. To provide more flexibility with various oxygenated products, the lumping group structure has been extended from 20 groups to 30 groups in this study. The model was evaluated using outdoor chamber data for the SOA produced from the photooxidation of toluene or 1,3,5-trimethylbenzene (135-TMB) in the presence and absence of SO_2 under varying NO_x conditions.

2 Experimental section

SOA formation from the photo-oxidation of aromatic volatile organic compounds (AV-OCs) (toluene or 135-TMB) with and without SO_2 under two different NO_x conditions were studied using the University of Florida Atmospheric PHotochemical Outdoor Reactor (UF-APHOR) dual chambers located on the roof of Black Hall (latitude/longitude: $29.64185^\circ/-82.347883^\circ$) at the University of Florida, Gainesville, Florida. The air volume of the two half-cylinder shaped, dual chambers is 104 m^3 ($52 \text{ m}^3 + 52 \text{ m}^3$) (Fig. S1). The dual, Teflon film chambers allow us to simultaneously conduct two experiments under the same meteorological conditions, e.g. sunlight, temperature and relative humidity. A detailed description of the chamber, experimental procedures, and instrumentation are shown in the Supplement (Sect. S1).

SOA formation was determined by measuring the organic carbon (OC) concentration (semi-continuous OC/EC carbon aerosol analyzer, Sunset Laboratory, Model 4). The OC is converted to OM by multiplying by the $[\text{OM}]/[\text{OC}]$ ratio (2.0), which is the

A model for aromatic SOA formation by multiphase reactions

Y. Im et al.

Title Page

Abstract

Introduction

Conclusions

References

Tables

Figures

◀

▶

◀

▶

Back

Close

Full Screen / Esc

Printer-friendly Version

Interactive Discussion



reported value for aromatic SOA (Izumi and Fukuyama, 1990). The SOA yield (Y) is calculated as the ratio of the formed OM to the reacted hydrocarbon concentration (ΔHC): $Y = \Delta\text{OM}/\Delta\text{HC}$ (Odum et al., 1996). In this study, the proton concentration ($[\text{H}^+]$, molL^{-1} in the inorganic aerosol) of aerosols was measured by two methods:

5 Particle into Liquid Sampler-Ion Chromatography (PILS-IC) with the inorganic thermodynamic model (E-AIM II) (Clegg et al., 1998) and the Colorimetry Integrated with a Reflectance UV-Visible Spectrometer (C-RUV) method (Jang et al., 2008). A detailed description of the acidity measurement using the C-RUV method is shown in the Supplement (Sect. S1). The $[\text{H}^+]$ estimated from PILS-IC data does not include the acidity

10 change by OS formation, while that from C-RUV data includes OS formation. The difference in $[\text{H}^+]$ between two methods is used to estimate OS (a detailed calculation of OS is described in Sect. S4 in Supplement).

3 Description of the UNIPAR model

Gas-phase chemistry treated by the Master Chemical Mechanism (MCM V3.2) (Jenkin et al., 2003; Bloss et al., 2005), an explicit gas-phase kinetic mechanism, provides the concentrations and chemical structures (functional groups) of oxidized products in the gas phase. To effectively account for wide ranges of complex atmospheric oxidized products, the model employs a lumping frame based on volatility of chemical species and reactivity for aerosol phase reaction. The aerosol phase concentrations of

15 each lumping group are estimated by a thermodynamic model (partitioning of lumping species between the gas (g), organic aerosol (or) and inorganic aerosol (in) phases) and then applied to aerosol phase reactions. The total organic matter (OM_T), SOA mass in the UNIPAR model is predicted by two modules: the module for organic matter (OM_P) by a partitioning process and the module for the OM (OM_{AR}) produced by

20 aerosol-phase reactions of organic compounds. Figure 1 illustrates how major processes in both the gas and aerosol phases are connected to SOA formation. In the following sections, the model components are described in detail in order of computation

25

in the UNIPAR model (from oxidation of AVOC to OM formation). The UNIPAR model was coded using Fortran.

3.1 Gas-phase chemistry

The oxidation of AVOC and the resulting oxygenated products are predicted using an explicit gas-kinetic mechanism (MCM V3.2) integrated with Morpho, a gas kinetic chemical solver (Jeffries and Kessler, 1998). The products predicted from the explicit gas-kinetic mechanisms provide the information required for both partitioning (product volatility distribution) and aerosol phase reactions (product reactivity) through the oxidized product molecular structures.

3.2 Product lumping structure

The oxygenated products produced from the MCM simulation are lumped into 30 groups based on their vapor pressures (6 levels: 10^{-8} , 10^{-6} , 10^{-5} , 10^{-4} , 10^{-3} , 10^{-2} mmHg) at 298 K and aerosol phase reaction reactivities (5 levels: fast F, medium M, slow S, non-reactive P and multi-alcohol MA). The lumped products are used to construct the mass based stoichiometric coefficients ($\alpha_{i,j}$) matrix, the major set of parameters used to describe the concentrations of organic compounds in multiphase as shown in Eq. (1) below.



where $L_{i,j}$ are lumping species. The detailed description of product lumping is shown in the Supplement (Sect. S5). The list of products for each lumping group for toluene and 135-TMB are shown in Figs. S6 and S7 in Supplement.

In the UNIPAR model, the dependence of aromatic SOA formation on NO_x was treated by parameterizing various product distributions under different NO_x conditions.

A model for aromatic SOA formation by multiphase reactions

Y. Im et al.

Title Page

Abstract

Introduction

Conclusions

References

Tables

Figures

◀

▶

◀

▶

Back

Close

Full Screen / Esc

Printer-friendly Version

Interactive Discussion



The photooxidations of toluene or 135-TMB were simulated over a range of VOC/NO_x ratios (ppbC/ppb, 4.5–90) using the MCM V3.2 (details in Sect. S6). Then, regression equations of $\alpha_{i,j}$ as functions of the VOC/NO_x ratio were obtained from the simulation results (Tables S5 and S6 in Supplement).

3.3 Product concentrations among gas, organic and inorganic aerosol phases

As shown in Fig. 1, the aerosol is assumed to have two separated liquid phases: the organic phase and the inorganic aqueous phase. Both laboratory and modeling studies (Clegg et al., 2001; Chang and Pankow, 2006; Ciobanu et al., 2009; Bertram et al., 2011; Song et al., 2012; Zuend and Seinfeld, 2012) have suggested that a liquid-liquid phase separation (the organic and electrolyte aqueous phases) in the ambient aerosols is favored rather than a homogeneously mixed single phase at moderate RH conditions. The estimation of concentrations ($\mu\text{g m}^{-3}$ of air) of lumping species, i in the gas phase ($C_{g,i}$), organic phase ($C_{or,i}$) and inorganic phase ($C_{in,i}$) is derived from two gas-particle partitioning coefficients, $K_{or,i}$ ($\text{m}^3 \mu\text{g}^{-1}$, $\text{g} \leftrightarrow \text{or}$) and $K_{in,i}$ ($\text{m}^3 \mu\text{g}^{-1}$, $\text{g} \leftrightarrow \text{in}$).

$$K_{or,i} = \frac{C_{or,i}}{C_{g,i} \text{OM}_T} \quad (2)$$

$$K_{in,i} = \frac{C_{in,i}}{C_{g,i} M_{in}} \quad (3)$$

where OM_T (SOA mass) is the total organic aerosol mass concentration ($\mu\text{g m}^{-3}$ of air) and M_{in} is the inorganic aerosol mass concentration ($\mu\text{g m}^{-3}$ of air). Both $K_{or,i}$ and $K_{in,i}$ are estimated using the Pankow's gas-particle absorption partition model (Eq. S1) (Pankow, 1994). In calculation of $K_{or,i}$, the activity coefficients ($\gamma_{or,i}$) of lumping species in the organic phase are assumed as unity (Jang and Kamens, 1998). Modeling efforts have been made to estimate activity coefficients ($\gamma_{in,i}$) of organic compounds in the inorganic aqueous phase (Zuend and Seinfeld, 2012), but the predictions are limited due

Title Page

Abstract

Introduction

Conclusions

References

Tables

Figures

◀

▶

◀

▶

Back

Close

Full Screen / Esc

Printer-friendly Version

Interactive Discussion



to the complexity of organic compounds and the lack of data base. So, in this study, $\gamma_{in,i}$ was semiempirically estimated. First, $\gamma_{in,i}$ was estimated under the saturated condition in pure water using Hansen's solubility parameter method (Barton, 1991) and was then corrected to the one in a salted aqueous phase at 70 % RH using an empirically obtained relationship between solubility of organic compounds in pure water and that in aqueous inorganic aerosol. For the solubility of organic compounds in inorganic aerosol, literature solubility data for NaCl aqueous solution were used because of the lack of literature data for SO₄-NH₄-water. Detailed estimation of the activity coefficient of lumping species in the inorganic aqueous phase is described in Supplement (Sect. S2).

The concentrations of each lumping species in the gas, organic aerosol, and inorganic aerosol-phases are derived from the Eqs. (2) and (3).

$$C_{g,i} = \frac{1}{1 + K_{or,i}OM_T + K_{in,i}M_{in}} C_{T,i} \quad (4)$$

$$C_{or,i} = \frac{K_{or,i}OM_T}{1 + K_{or,i}OM_T + K_{in,i}M_{in}} C_{T,i} \quad (5)$$

$$C_{in,i} = \frac{K_{in,i}M_{in}}{1 + K_{or,i}OM_T + K_{in,i}M_{in}} C_{T,i} \quad (6)$$

where $C_{T,i}$ ($\mu\text{g m}^{-3}$ of air, $C_{T,i} = C_{g,i} + C_{or,i} + C_{in,i}$) is the total concentration of lumping species i . The resulting $C_{or,i}$ and $C_{in,i}$ are applied to the calculation of OM_{AR} through aerosol phase reactions as shown in the next section.

3.4 SOA formation (OM_{AR}) by aerosol-phase reactions

OM_{AR} is described by two processes: (1) the oligomerization reaction in the organic-phase and (2) the acid-catalyzed reaction in the inorganic-phase. The reactions in both the organic phase (Eq. 7) and inorganic phase (Eq. 8) are derived based on a second

A model for aromatic SOA formation by multiphase reactions

Y. Im et al.

Title Page

Abstract

Introduction

Conclusions

References

Tables

Figures

◀

▶

◀

▶

Back

Close

Full Screen / Esc

Printer-friendly Version

Interactive Discussion



The amount of OM ($\Delta\text{OM}_{\text{AR}}$) formed by aerosol-phase reactions is same as the consumption of the total concentration of compound ($-\Delta C_{\text{T}}$) based on a mass balance. Therefore, the $\Delta\text{OM}_{\text{AR}}$ can be expressed as

$$\Delta\text{OM}_{\text{AR}} = - \sum_i \Delta C_{\text{T},i} = \sum_i \int dC_{\text{T},i} \quad (10)$$

5 By combining Eqs. (2)–(8), the kinetic equation of $C_{\text{T},i}$ can be expressed as follows. (The detailed derivation is shown in Supplement, Sect. S3).

$$\frac{dC_{\text{T},i}}{dt} = -k_{\text{o},i} C_{\text{or},i}^2 \left(\frac{MW_i \text{OM}_{\text{T}}}{\rho_{\text{or}} 10^3} \right) - k_{\text{AC},i} C_{\text{in},i}^2 \left(\frac{MW_i M_{\text{in}}}{\rho_{\text{in}} 10^3} \right) \quad (11)$$

10 where ρ_{or} and ρ_{in} are the densities of the organic and inorganic aerosol phases, respectively. OM_{AR} is estimated from the analytical solution of Eq. (11) in the UNIPAR model.

3.5 Change of aerosol acidity by OS formation

The reaction of organic species with sulfuric acid to form OS decreases aerosol acidity. This change can affect the acid-catalyzed reaction for SOA formation, requiring an estimation of the acidity change by OS formation. In the model, the removal of a sulfate ion by OS formation (OS conversion factor based on available free sulfate, $[\text{SO}_4^{2-}]_{\text{free}}$) is estimated using Eq. (12) at each time step (Fig. 2).

$$\text{OS conversion factor} = \frac{[\text{SO}_4^{2-}]_{\text{old}} - [\text{SO}_4^{2-}]_{\text{new}}}{[\text{SO}_4^{2-}]_{\text{old}}} = \frac{\Delta\text{OS}}{[\text{SO}_4^{2-}]_{\text{old}}} = 1 - \frac{1}{1 + f_{\text{OS}} \frac{N_{\text{OS}}}{[\text{SO}_4^{2-}]_{\text{free}}}} \quad (12)$$

20 where $[\text{SO}_4^{2-}]_{\text{old}}$ and $[\text{SO}_4^{2-}]_{\text{new}}$ are sulfate concentrations (molL^{-1} of inorganic aerosol) before and after sulfate consumption by OS formation, respectively. Before the formation of new OS at each time step, $[\text{SO}_4^{2-}]_{\text{free}}$ (molL^{-1} of inorganic aerosol), which can

Title Page

Abstract

Introduction

Conclusions

References

Tables

Figures

◀

▶

◀

▶

Back

Close

Full Screen / Esc

Printer-friendly Version

Interactive Discussion



A model for aromatic SOA formation by multiphase reactions

Y. Im et al.

Title Page

Abstract

Introduction

Conclusions

References

Tables

Figures

◀

▶

◀

▶

Back

Close

Full Screen / Esc

Printer-friendly Version

Interactive Discussion



form OS, is calculated by excluding a sulfate ion in ammonium sulfate from the total ionic sulfate $[\text{SO}_4^{2-}]_{\text{ion}}$ that is not associated with OS: $[\text{SO}_4^{2-}]_{\text{free}} = [\text{SO}_4^{2-}]_{\text{ion}} - 0.5[\text{NH}_4^+]$. N_{OS} is the parameter to count the functional groups that can react with sulfate to form OS. Aldehyde, epoxide and alcohol groups are counted as the OS-formable functional groups because of their reactivity with sulfate. The semiempirical parameter f_{OS} is obtained by comparison of acidity measurements and model simulations. A detailed calculation of N_{OS} and a description of f_{OS} are shown in the Supplement (Sect. S4). When N_{OS} is very high, ΔOS becomes high at a given $[\text{SO}_4^{2-}]_{\text{free}}$. When N_{OS} is very small, the OS conversion factor is nearly zero. Based on the inorganic species from the previous time step (except OS sulfates) and the new ionic species added into the system, both $a_{\text{in,w}}$ and $[\text{H}^+]$ are calculated at each time step using the inorganic thermodynamic model. The new $a_{\text{in,w}}$ and $[\text{H}^+]$ are applied to Eq. (9) for estimating $k_{\text{AC},i}$.

3.6 SOA formation by partitioning (OM_P)

The OM_P is estimated using the SOA partitioning module derived by Schell et al. (2001) that has been employed in CMAQ. In the UNIPAR model, the OM_P module has been modified by inclusion of OM_{AR} (Cao and Jang, 2010) based on a mass balance of organic compounds between the gas and particle phases. After calculation of OM_{AR} , $C_{g,i}$ and $C_{\text{or},i}$ are recalculated numerically using Eq. (13) (Press et al., 1992)

$$\text{OM}_P = \sum_i C_{\text{or},i} = \sum_i \left[C_{\text{T},i} - \text{OM}_{\text{AR},i} - C_{g,i}^* \frac{\frac{C_{\text{or},i}}{\text{MW}_i}}{\sum_k \left(\frac{C_{\text{or},k}}{\text{MW}_k} + \frac{\text{OM}_{\text{AR}}}{\text{MW}_{\text{oli}}} + \text{OM}_0 \right)} \right] \quad (13)$$

where $C_{g,i}^*$ is the saturated gas-phase concentration of lumping species, i , MW_k is the molecular weight of lumping species, k and MW_{oli} is the average molecular weight of oligomers formed from aerosol-phase reactions. OM_0 is the mass concentration of preexisting organic particular matter (mol m^{-3}). The estimations of $C_{g,i}$ and $C_{\text{or},i}$ by

Eqs. (4)–(6) are approached those by the OM_P module since $K_{in,i}M_{in}$ in the denominators of Eqs. (4)–(6) is relatively very small compared to $K_{or,i}OM_T$.

3.7 Model simulation

To estimate SOA formation over time under dynamically changing environmental conditions such as temperature, RH, and inorganic aerosol composition and mass, the model calculates SOA mass at each time interval ($\Delta t = 3$ min) by updating the input parameters. In this study, five input parameters were used: decay of precursor AVOC (ΔROG) (from MCM simulation), increments of sulfate (ΔSO_4) and ammonium (ΔNH_4) ion concentration (from PILS-IC), temperature and RH.

4 Result and discussion

4.1 Gas-phase model simulation vs. experimental data

According to previous studies (Wagner et al., 2003; Johnson et al., 2004; Bloss et al., 2005), the kinetic mechanisms of aromatic hydrocarbons in MCM overestimate ozone peaks and underestimate precursor decay due to the low production of OH radicals. Hence, an artificial OH radical was added to the toluene mechanism in this study. The artificial OH radical production rate was determined by comparing the simulated toluene decay to the measured data. The OH radical production rate for the toluene mechanism of this study was approximately 2.0×10^8 molecules $cm^3 s^{-1}$, which is smaller than previously reported values ($\sim 4.0 \times 10^8$ molecules $cm^3 s^{-1}$) (Bloss et al., 2005; Cao and Jang, 2010). The discrepancy between the artificial OH radical production rate of this study and those previously published may be attributed to different experimental conditions such as initial VOC (200 ppb vs. 700 ppb) and NO_x concentrations as well as meteorological conditions. In the same manner, the production rate of artificial OH radicals for the 135-TMB mechanism was 1.7×10^8 molecules $cm^3 s^{-1}$.

A model for aromatic SOA formation by multiphase reactions

Y. Im et al.

Title Page

Abstract

Introduction

Conclusions

References

Tables

Figures

◀

▶

◀

▶

Back

Close

Full Screen / Esc

Printer-friendly Version

Interactive Discussion



A model for aromatic SOA formation by multiphase reactions

Y. Im et al.

Title Page

Abstract

Introduction

Conclusions

References

Tables

Figures

◀

▶

◀

▶

Back

Close

Full Screen / Esc

Printer-friendly Version

Interactive Discussion



Toluene experiments were conducted for 12 h (07:00–17:00 EST), but 135-TMB experiments could only be conducted for 5 h (07:00–12:00 EST) because of the fast reactivity of 135-TMB (all 135-TMB was consumed before 12:00 EST). Overall, VOC decay, NO/NO₂ conversion and O₃ production are reasonably predicted. The comparison of gas-phase experimental data with simulation results for toluene and 135-TMB in two different NO_x conditions was shown in Fig. S2 (Supplement).

It is well known that SO₂ can be oxidized through both gas-phase reactions with OH radicals and heterogeneous chemistry on the aqueous surface (aerosol and chamber wall). Due to the lack of the heterogeneous reaction mechanisms for the oxidation of SO₂, sulfuric acid was not predicted by an explicit mechanism. The sulfate concentrations measured by PILS-IC were directly applied to the UNIPAR model to simulate the effect of inorganic species on SOA formation.

4.2 Effect of NO_x on aromatic SOA formation

Fig. 3 shows model simulations of both toluene SOA (Fig. 3a, b) and 135-TMB SOA (Fig. 3c, d) against experimental data with and without SO₂ under two different NO_x levels. The yields of toluene and 135-TMB SOA were determined at 14:00 EST and 11:00 EST, respectively. For toluene, SOA yields under the lower NO_x condition (Fig. 3a, 18.9% with and 13.3% without SO₂) were higher than those under the higher NO_x condition (Fig. 3b, 15.3% with and 9.3% without SO₂). This trend is consistent with other studies (Ng et al., 2007; Kroll et al., 2007). Overall, the UNIPAR model reasonably predicted measured OM concentrations of both high and low NO_x conditions. However, during the later part of the study (after 15:00 EST), the model tends to overestimate the measured OM concentrations. This may be due to the hypersensitivity to temperature in the model and the adsorption of SVOCs to chamber walls at low temperatures. When the toluene chamber experiments were conducted (January–February), chamber temperature decreased sharply after 15:00 EST (Fig. S8). Furthermore, to evaluate the model performance in a wider range of NO_x levels, toluene SOA was

simulated in various NO_x levels (VOC/NO_x ratio: 2–84, ppbC/ppb) and the simulation results showed a consistent trend with other laboratory studies (Fig. S9).

The trend of 135-TMB SOA yields is opposite of the toluene SOA yields, showing higher SOA yields under higher NO_x conditions (7.3% with SO₂, 4.9% without SO₂) than those under lower NO_x conditions (5.7% with SO₂, 3.4% without SO₂). This result appears inconsistent with previous studies (Wyche et al., 2008). This discrepancy may be partially explained by differences in environmental conditions among different chambers and aerosol aging. Overall, the OM model accorded well with 135-TMB experiments in the presence of SO₂, but without SO₂ the UNIPAR model underestimates OM compared to experimental data (Fig. 3c, d). The deviation of model prediction from observation can be caused by the uncertainty of the $\alpha_{i,j}$ matrix, which is affected by the reaction time. The actual 135-TMB SOA might be produced from more aged products than that used in the model, where the $\alpha_{i,j}$ matrix is determined at the half of 135-TMB consumption.

4.3 Organosulfate formation

The UNIPAR model estimates the formation of OS using the amount of consumed sulfate (SO₄²⁻) estimated by Eq. (12) and the average molecular weight of OS products. The average molecular weight of OS, which changes dynamically depending on the change of the OM_{AR} matrix over the course of the experiment, was predicted by the model. The predicted OS fraction of the total OM (OS/OM_T) from the model is illustrated in Fig. 5a for both toluene SOA and 135-TMB SOA under two different NO_x conditions. In this study, the fractions of OS of the total OM (OS/OM_T) were 0.095 for toluene SOA under the low NO_x condition and 0.052 under the high NO_x condition. For 135-TMB SOA, the fraction of OS (OS/OM_T) was 0.076 with the low NO_x condition and 0.077 with the high NO_x condition. The predicted OS fractions of the total sulfates ($[\text{SO}_4^{2-}]_{\text{OS}}/[\text{SO}_4^{2-}]_{\text{total}}$) from the model reasonably agreed with experimentally measured values using the C-RUV and PILS-IC data (Fig. 5b).

A model for aromatic SOA formation by multiphase reactions

Y. Im et al.

Title Page

Abstract

Introduction

Conclusions

References

Tables

Figures

◀

▶

◀

▶

Back

Close

Full Screen / Esc

Printer-friendly Version

Interactive Discussion



4.4 Effect of inorganic aerosol acidity on aromatic SOA formation

Sulfuric acid produced from the oxidation of SO_2 is neutralized by ammonia gas present in the background chamber air, forming an inorganic aerosol consisting of sulfate, ammonia and water. Hence, the mass concentrations and the compositions of inorganic aerosols dynamically changed over the course of the chamber experiments.

SOA yields were higher in the presence of SO_2 than without SO_2 for all toluene and 135-TMB experiments, because the acidic inorganic aerosol is attributed to an increased OM through acid-catalyzed reactions. For example, with SO_2 , toluene SOA yields increased by 42 % under the low NO_x condition and by 65 % under the high NO_x condition (Table 1 and Fig. 3). 135-TMB increased by 68 % under the low NO_x conditions and by 49 % under the high NO_x condition. As shown in Fig. 3, the model also reasonably predicted acidity effects on both toluene and 135-TMB SOA. Particularly, SOA mass predictions were improved by the inclusion of aerosol acidity reduction (due to the OS formation) in the model.

The sensitivity of toluene SOA to aerosol acidity was also simulated using the UNIPAR model. For model simulation, toluene was oxidized under the two different %RH (30 and 60) in the presence of four different inorganic aerosols: sulfuric acid (SA), ammonium bisulfate (ABS), ammonium sulfate (AS), and neutralization of sulfuric acid aerosol with ammonia (SA to AS) as shown in Fig. 4. At the lower humidity (%RH = 30), the SOA production is the highest with SA, followed by ABS and the lowest with AS. At the higher humidity (%RH = 60, RH > ERH of AS), the acidity effect on SOA production becomes weak compared to that in the lower humidity. There is almost no difference in SOA production between the ABS system and the AS system. The OS products formed in both SA and ABS systems are hydrophobic and influence the hygroscopic properties of inorganic aerosols. The reduction of water content due to OS formation can suppress the formation of SOA through acid-catalyzed reactions in aqueous phase.

ACPD

13, 5843–5870, 2013

A model for aromatic SOA formation by multiphase reactions

Y. Im et al.

Title Page

Abstract

Introduction

Conclusions

References

Tables

Figures

◀

▶

◀

▶

Back

Close

Full Screen / Esc

Printer-friendly Version

Interactive Discussion



5 Model uncertainty and implications

The major parameters of the UNIPAR model, such as product stoichiometric coefficient ($\alpha_{i,j}$), vapor pressure, and aerosol phase reaction reactivity, were determined from the simulation results of the explicit gas-phase mechanisms (e.g. MCM). Thus, the capability for accurate predictions of oxygenated products using the explicit kinetic mechanisms directly influences the performance of the UNIPAR model. Most kinetic mechanisms of photooxidation of aromatic hydrocarbons have not been tested due to the lack of authentic standards. For example, in a recent study by Sato et al. (2007), the toluene oxygenated products are identified as only 1 wt% of total organic mass. In this study, the addition of artificial OH radicals in the mechanisms suggests that the explicit gas-kinetic mechanisms for aromatic VOCs need further development. Although the $\alpha_{i,j}$ matrix was described considering a VOC/NO_x ratio and applied to dynamically express aerosol phase reactions, the $\alpha_{i,j}$ matrix was not determined as a function of time at a given NO_x condition. Thus, the $\alpha_{i,j}$ matrix is limited in expressing the dynamically changing gas-phase composition as gas-phase products photochemically age. The estimation of the activity coefficients of organic compounds in the salted aqueous phase is also uncertain due to the lack of data sets of solubility of organic compounds in various inorganic salt solutions.

In current study, the UNIPAR model included new aerosol phase reactions such as OS formation and improved the prediction of aromatic SOA formation under various aerosol acidities, NO_x concentrations, humidities and temperatures. Particularly, the UNIPAR model would improve the prediction of SOA in the urban atmosphere, where acidic inorganic aerosols are abundant (through the oxidation of SO₂). Furthermore, the product lumping structure ($\alpha_{i,j}$), based on volatility and reactivity, and universal aerosol-phase reaction rate constants in the model can be applied to various SOA systems produced from different VOCs. In order to apply the UNIPAR model to the regional scale air quality model, the model parameters need to be tested for various SOAs that

ACPD

13, 5843–5870, 2013

A model for aromatic SOA formation by multiphase reactions

Y. Im et al.

Title Page

Abstract

Introduction

Conclusions

References

Tables

Figures

◀

▶

◀

▶

Back

Close

Full Screen / Esc

Printer-friendly Version

Interactive Discussion



originate from different anthropogenic and biogenic VOCs as well as a mixture of several VOCs under ambient relevant conditions.

Supplementary material related to this article is available online at:

<http://www.atmos-chem-phys-discuss.net/13/5843/2013/>

[acpd-13-5843-2013-supplement.pdf](#)

Acknowledgements. This work was supported by a Grant from National Science Foundation (ATM-0852747) and a Navy (N61331-11-1-G001).

References

Barton, A. F. M.: CRC Handbook of Solubility Parameters and Other Cohesion Parameters, 2nd edn., CRC Press. Inc., Boca Raton, 1991. 5851

Bäumer, D., Vogel, B., Versick, S., Rinke, R., Möhler, O., and Schnaiter, M.: Relationship of visibility, aerosol optical thickness and aerosol size distribution in an ageing air mass over South-West Germany, *Atmos. Environ.*, 42, 989–998, 2008. 5844

Bertram, A. K., Martin, S. T., Hanna, S. J., Smith, M. L., Bodsworth, A., Chen, Q., Kuwata, M., Liu, A., You, Y., and Zorn, S. R.: Predicting the relative humidities of liquid-liquid phase separation, efflorescence, and deliquescence of mixed particles of ammonium sulfate, organic material, and water using the organic-to-sulfate mass ratio of the particle and the oxygen-to-carbon elemental ratio of the organic component, *Atmos. Chem. Phys.*, 11, 10995–11006, doi:10.5194/acp-11-10995-2011, 2011. 5850

Betterton, E. A. and Hoffmann, M. R.: Kinetics, mechanism, and thermodynamics of the reversible reaction of methylglyoxal with S(IV), *J. Phys. Chem.*, 91, 3011–3020, 1987. 5845

Bloss, C., Wagner, V., Jenkin, M. E., Volkamer, R., Bloss, W. J., Lee, J. D., Heard, D. E., Wirtz, K., Martin-Reviejo, M., Rea, G., Wenger, J. C., and Pilling, M. J.: Development of a detailed chemical mechanism (MCMv3.1) for the atmospheric oxidation of aromatic hydrocarbons, *Atmos. Chem. Phys.*, 5, 641–664, doi:10.5194/acp-5-641-2005, 2005. 5848, 5855

ACPD

13, 5843–5870, 2013

A model for aromatic SOA formation by multiphase reactions

Y. Im et al.

Title Page

Abstract

Introduction

Conclusions

References

Tables

Figures

◀

▶

◀

▶

Back

Close

Full Screen / Esc

Printer-friendly Version

Interactive Discussion



A model for aromatic SOA formation by multiphase reactions

Y. Im et al.

Title Page

Abstract

Introduction

Conclusions

References

Tables

Figures

◀

▶

◀

▶

Back

Close

Full Screen / Esc

Printer-friendly Version

Interactive Discussion



- Cao, G. and Jang, M.: Effects of particle acidity and UV light on secondary organic aerosol formation from oxidation of aromatics in the absence of NO_x , *Atmos. Environ.*, 41, 7603–7613, 2007. 5845
- Cao, G. and Jang, M.: An SOA model for toluene oxidation in the presence of inorganic aerosols, *Environ. Sci. Technol.*, 44, 727–733, 2010. 5845, 5846, 5854, 5855
- Cappa, C. D. and Wilson, K. R.: Multi-generation gas-phase oxidation, equilibrium partitioning, and the formation and evolution of secondary organic aerosol, *Atmos. Chem. Phys.*, 12, 9505–9528, doi:10.5194/acp-12-9505-2012, 2012. 5846
- Chang, E. I. and Pankow, J. F.: Prediction of activity coefficients in liquid aerosol particles containing organic compounds, dissolved inorganic salts, and water – part 2: consideration of phase separation effects by an X-UNIFAC model, *Atmos. Environ.*, 40, 6422–6436, 2006. 5850
- Ciobanu, V. G., Marcolli, C., Krieger, U. K., Weers, U., and Peter, T.: Liquid-liquid phase separation in mixed organic/inorganic aerosol particles, *J. Phys. Chem. A*, 113, 10966–10978, 2009. 5850
- Clegg, S. L., Brimblecombe, P., and Wexler, A. S.: A thermodynamic model of the system $\text{H}^+ - \text{NH}_4^+ - \text{SO}_4^{2-} - \text{NO}_3^- - \text{H}_2\text{O}$ at tropospheric temperatures, *J. Phys. Chem. A*, 102, 2137–2154, 1998. 5848, 5852
- Clegg, S. L., Seinfeld, J. H., and Brimblecombe, P.: Thermodynamic modelling of aqueous aerosols containing electrolytes and dissolved organic compounds, *J. Aerosol. Sci.*, 32, 713–738, 2001. 5850
- Colberg, C. A., Luo, B. P., Wernli, H., Koop, T., and Peter, Th.: A novel model to predict the physical state of atmospheric $\text{H}_2\text{SO}_4/\text{NH}_3/\text{H}_2\text{O}$ aerosol particles, *Atmos. Chem. Phys.*, 3, 909–924, doi:10.5194/acp-3-909-2003, 2003. 5852
- Czochke, N. M., Jang, M., and Kamens, R. M.: Effect of acidic seed on biogenic secondary organic aerosol growth, *Atmos. Environ.*, 37, 4287–4299, 2003. 5845
- Darer, A. I., Cole-Filipiak, N. C., O'Connor, A. E., and Elrod, M. J.: Formation and stability of atmospherically relevant isoprene-derived organosulfates and organonitrates, *Environ. Sci. Technol.*, 45, 1895–1902, 2011. 5845
- Donahue, N. M., Robinson, A. L., and Pandis, S.: Coupled partitioning, dilution, and chemical aging of semivolatile organics, *Environ. Sci. Technol.*, 40, 2635–2643, 2006. 5845
- Galloway, M. M., Chhabra, P. S., Chan, A. W. H., Surratt, J. D., Flagan, R. C., Seinfeld, J. H., and Keutsch, F. N.: Glyoxal uptake on ammonium sulphate seed aerosol: reaction products and

A model for aromatic SOA formation by multiphase reactions

Y. Im et al.

Title Page

Abstract

Introduction

Conclusions

References

Tables

Figures

◀

▶

◀

▶

Back

Close

Full Screen / Esc

Printer-friendly Version

Interactive Discussion



reversibility of uptake under dark and irradiated conditions, *Atmos. Chem. Phys.*, 9, 3331–3345, doi:10.5194/acp-9-3331-2009, 2009. 5845

Garland, R. M., Elrod, M. J., Kincaid, K., Beaver, M. R., Jimenez, J. L., and Tolbert, M. A.: Acid-catalyzed reactions of hexanal on sulfuric acid particles: identification of reaction products, *Atmos. Environ.*, 40, 6863–6878, 2006. 5845

Imuma, Y., Boge, O., Gnauk, T., and Hermann, H.: Aerosol-chamber study of the α -pinene/O₃ reaction: influence of particle acidity on aerosol yields and products, *Atmos. Environ.*, 38, 761–773, 2004. 5845

IPCC: Intergovernmental Panel on Climate Change (IPCC): *Climate change: the Scientific Basis*, Cambridge University Press, 2001. 5844

Izumi, K. and Fukuyama, T.: Photochemical aerosol formation from aromatic hydrocarbons in the presence of NO_x, *Atmos. Environ.*, 24, 1433–1490, 1990. 5848

Jang, M. and Kamens, R. M.: A thermodynamic approach for modeling partitioning of semivolatile organic compounds on atmospheric particulate matter: humidity effects, *Environ. Sci. Technol.*, 32, 1237–1243, 1998. 5850

Jang, M. and Kamens, R. M.: Atmospheric secondary aerosol formation by heterogeneous reactions of aldehydes in the presence of a sulfuric acid aerosol catalyst, *Environ. Sci. Technol.*, 35, 4758–4766, 2001. 5845

Jang, M., Czoschke, N. M., Northcross, A. L., Cao, G., and Shaof, D.: SOA formation from partitioning and heterogeneous reactions: model study in the presence of inorganic species, *Environ. Sci. Technol.*, 40, 3013–3022, 2006. 5846, 5852

Jang, M., Cao, G., and Jared, P.: Acidity measurement of atmospheric aerosol by a colorimetric analysis, *Aerosol Sci. Technol.*, 42, 409–420, 2008. 5848

Jeffries, H. E. and Kessler, M.: *Morphocycle/Allomorph Reaction Mechanisms*, Final report to U.S. EPA, contract 68D50129, 1999. 5849

Jenkin, M. E., Saunders, S. M., Wagner, V., and Pilling, M. J.: Protocol for the development of the Master Chemical Mechanism, MCM v3 (Part B): tropospheric degradation of aromatic volatile organic compounds, *Atmos. Chem. Phys.*, 3, 181–193, doi:10.5194/acp-3-181-2003, 2003. 5848

Johnson, D., Jenkin, M. E., Wirtz, K., and Martin-Reviejo, M.: Simulating the formation of secondary organic aerosol from the photooxidation of toluene, *Environ. Chem.*, 1, 150–165, 2004. 5855

A model for aromatic SOA formation by multiphase reactions

Y. Im et al.

Title Page

Abstract

Introduction

Conclusions

References

Tables

Figures

◀

▶

◀

▶

Back

Close

Full Screen / Esc

Printer-friendly Version

Interactive Discussion



- Kamens, R., Jang, M., Chien, C. J., and Leach, K.: Aerosol formation from the reaction of α -pinene and ozone using a gas-phase kinetics-aerosol partitioning model, *Environ. Sci. Technol.*, 33, 1430–1438, 1999. 5846
- 5 Kleindienst, T. E., Edney, E. O., Lewandowski, M., Offenberg, J. H., and Jaoui, M.: Secondary organic carbon and aerosol yields from the irradiations of isoprene and α -pinene in the presence of NO_x and SO_2 , *Environ. Sci. Technol.*, 40, 3807–3812, 2006. 5845
- Kleinman, L. I., Springston, S. R., Daum, P. H., Lee, Y.-N., Nunnermacker, L. J., Senum, G. I., Wang, J., Weinstein-Lloyd, J., Alexander, M. L., Hubbe, J., Ortega, J., Canagaratna, M. R., and Jayne, J.: The time evolution of aerosol composition over the Mexico City plateau, *Atmos. Chem. Phys.*, 8, 1559–1575, doi:10.5194/acp-8-1559-2008, 2008. 5846
- 10 Kroll, J., Chan, A. W. H., Ng, N. L., Flagan, R. C., and Seinfeld, J. H.: Reactions of semivolatile organics and their effects on secondary organic aerosol formation, *Environ. Sci. Technol.*, 41, 3545–3550, 2007. 5856
- Ku, H.: Notes on the use of propagation of error formulas, *J. Res. Natl. B. Stand.*, 70, 263–273, 1966. 5865, 5870
- 15 Liggio, J., Li, S.-M., and McLaren, R.: Heterogeneous reaction of glyoxal on particulate matter: identification of acetals and sulfate esters, *Environ. Sci. Technol.*, 39, 1532–1541, 2005. 5845
- Ng, N. L., Kroll, J. H., Chan, A. W. H., Chhabra, P. S., Flagan, R. C., and Seinfeld, J. H.: Secondary organic aerosol formation from *m*-xylene, toluene, and benzene, *Atmos. Chem. Phys.*, 7, 3909–3922, doi:10.5194/acp-7-3909-2007, 2007. 5856
- 20 Odum, J. R., Hoffmann, T., Bowman, F. A., Collins, D., Flagan, R. C., and Seinfeld, J. H.: Gas/particle partitioning and secondary organic aerosol yields, *Environ. Sci. Technol.*, 30, 2580–2585, 1996. 5845, 5848
- Olson, C. N., Galloway, M. M., Yu, G., Hedman, C. J., Lockett, M. R., Yoon, T., Stone, E. A., Smith, L. M., and Keutsch, F. N.: Hydroxycarboxylic acid-derived organosulfates: synthesis, stability, and quantification in ambient aerosol, *Environ. Sci. Technol.*, 45, 6468–6474, 2011. 5845
- 25 Pankow, J.: absorption model of gas/particle partitioning of organic compounds in the atmosphere, *Atmos. Environ.*, 28, 185–188, 1994. 5850
- 30 Press, W. H., Teukolsky, S. A., Vetterling, T. W., and Flannery, B. P.: *Numerical Recipes in Fortran 77*, 2nd edn., Cambridge University Press, New York, 1992. 5854

A model for aromatic SOA formation by multiphase reactions

Y. Im et al.

Title Page

Abstract

Introduction

Conclusions

References

Tables

Figures

◀

▶

◀

▶

Back

Close

Full Screen / Esc

Printer-friendly Version

Interactive Discussion



Sato, K., Hatakeyama, S., and Imamura, T.: Secondary organic aerosol formation during the photooxidation of toluene: NO_x dependence of chemical composition, *J. Phys. Chem. A*, 111, 9796–9808, 2007. 5859

Schell, B., Ackermann, I. J., Hass, H., Binkowski, F. S., and Ebel, A.: Modeling the formation of secondary organic aerosol within a comprehensive air quality model system, *J. Geophys. Res.*, 106, 28275–28293, 2001. 5854

Schwartz, J., Dockery, D. W., and Neas, L. M.: Is daily mortality associated specifically with fine particles, *J. Air Waste Manage. Assoc.*, 46, 927–939, 1996. 5844

Simpson, D., Yttri, K. E., Klimont, Z., Kupiainen, K., Caseiro, A., Gelencser, A., Pio, C., Puxbaum, H., and Legrand, M.: Modeling carbonaceous aerosol over Europe: analysis of CARBOSOL and EMEP EC/OC campaigns, *J. Geophys. Res.*, 112, D23S14, doi:10.1029/2006JD008158, 2007. 5846

Song, M., Marcolli, C., Krieger, U. K., Zuend, A., and Peter, T.: Liquid-liquid phase separation and morphology of internally mixed dicarboxylic acids/ammonium sulfate/water particles, *Atmos. Chem. Phys.*, 12, 2691–2712, doi:10.5194/acp-12-2691-2012, 2012. 5850

Surratt, J. D., Lewandowski, M., Offenberg, J. H., Jaoui, M., Kleindienst, T. E., Edney, E. O., and Seinfeld, J. H.: Effect of acidity on secondary organic aerosol formation from isoprene., *Environ. Sci. Technol.*, 41, 5363–5369, 2007. 5845

Wagner, V., Jenkin, M. E., Saunders, S. M., Stanton, J., Wirtz, K., and Pilling, M. J.: Modelling of the photooxidation of toluene: conceptual ideas for validating detailed mechanisms, *Atmos. Chem. Phys.*, 3, 89–106, doi:10.5194/acp-3-89-2003, 2003. 5855

Wyche, K. P., Monks, P. S., Ellis, A. M., Cordell, R. L., Parker, A. E., Whyte, C., Metzger, A., Dommen, J., Duplissy, J., Prevot, A. S. H., Baltensperger, U., Rickard, A. R., and Wulfert, F.: Gas phase precursors to anthropogenic secondary organic aerosol: detailed observations of 1,3,5-trimethylbenzene photooxidation, *Atmos. Chem. Phys.*, 9, 635–665, doi:10.5194/acp-9-635-2009, 2009. 5857

Zuend, A. and Seinfeld, J. H.: Modeling the gas-particle partitioning of secondary organic aerosol: the importance of liquid-liquid phase separation, *Atmos. Chem. Phys.*, 12, 3857–3882, doi:10.5194/acp-12-3857-2012, 2012. 5850

A model for aromatic SOA formation by multiphase reactions

Y. Im et al.

Table 1. SOA chamber experimental conditions and resulting SOA data.

NO.	Experiment	AVOC	Initial AVOC (ppb)	Initial NO (ppb)	Initial NO ₂ (HONO) (ppb)	VOC/NO _x (ppbC ppb ⁻¹)	Initial SO ₂ (ppb)	SOA yield ^b (%)	RH (%)	Temp. (K)
1	01/06/12 E	Toluene	190	35	35(40)	12.09	50	18.9 ± 1.7	81–18	280–306
2	01/06/12 W	Toluene	190	40	20(35)	14.78	–	13.3 ± 1.2	81–18	280–306
3	02/09/12 E	Toluene	175	180	30(35)	5.00	46	15.3 ± 1.4	83–21	280–307
4	02/09/12 W	Toluene	180	180	31(35)	4.52	–	9.3 ± 0.8	83–21	280–307
5	05/18/12 E	135-TMB	160	195	48(75)	5.14	–	4.9 ± 0.4	95–14	290–317
6	05/18/12 W	135-TMB	170	206	16(75)	6.06	40	7.3 ± 0.7	95–14	290–317
7	05/20/12 E	135-TMB	165	105	8(20)	11.12	–	3.4 ± 0.3	90–13	290–317
8	05/20/12 W	135-TMB	165	100	7(15)	12.12	43	5.7 ± 0.5	90–13	290–317
9	06/20/12 E	Toluene	165	90	5(15)	10.50	35 ^c	15.6 ± 1.4	83–27	295–317

^a E and W denote the east and west chamber.

^b SOA yields are determined at 14:00 EST for toluene, 11:00 EST for 135-TMB and the uncertainties of SOA yields are estimated from the uncertainties of OM and Δ ROG by the propagation of uncertainty (Ku, 1966).

^c Mass concentration of inorganic seed (sulfuric acid) ($\mu\text{g m}^{-3}$).

Title Page

Abstract

Introduction

Conclusions

References

Tables

Figures

◀

▶

◀

▶

Back

Close

Full Screen / Esc

Printer-friendly Version

Interactive Discussion



A model for aromatic SOA formation by multiphase reactions

Y. Im et al.

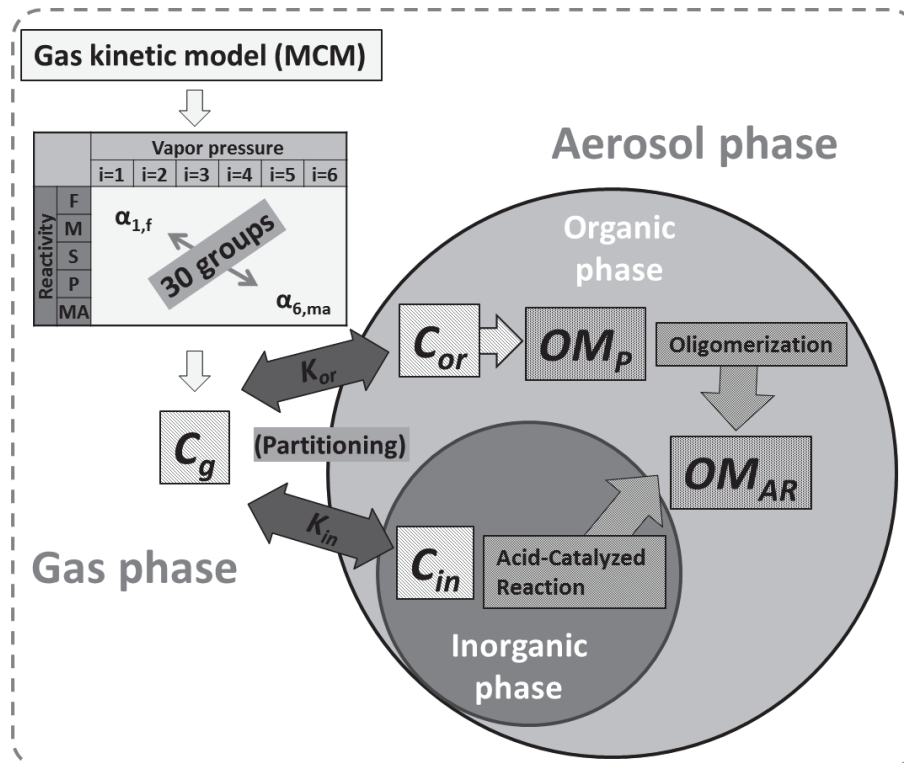


Fig. 1. Conceptual structure of the UNIPAR model.

Title Page

Abstract Introduction

Conclusions References

Tables Figures

⏪ ⏩

⏴ ⏵

Back Close

Full Screen / Esc

Printer-friendly Version

Interactive Discussion



A model for aromatic SOA formation by multiphase reactions

Y. Im et al.

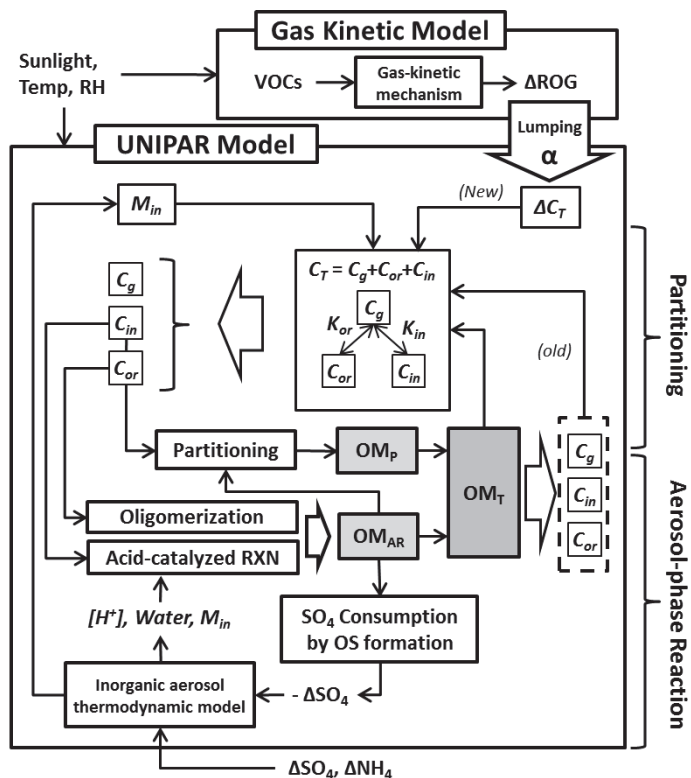


Fig. 2. Computational flow of the UNIPAR model. ΔROG is the reacted organic parent compound during Δt and $\alpha_{i,j}$ is the mass based stoichiometric coefficient. C and K represent the concentration of lumping species and partitioning coefficient, respectively, and the subscript of g, or, and in denote gas, organic, and inorganic aerosol phases, respectively. OM_p , and OM_{AR} are the concentrations of organic matter produced by partitioning and aerosol phase reactions, respectively. M_{in} is the concentration of inorganic aerosol.

Title Page

Abstract Introduction

Conclusions References

Tables Figures

◀ ▶

◀ ▶

Back Close

Full Screen / Esc

Printer-friendly Version

Interactive Discussion



A model for aromatic SOA formation by multiphase reactions

Y. Im et al.

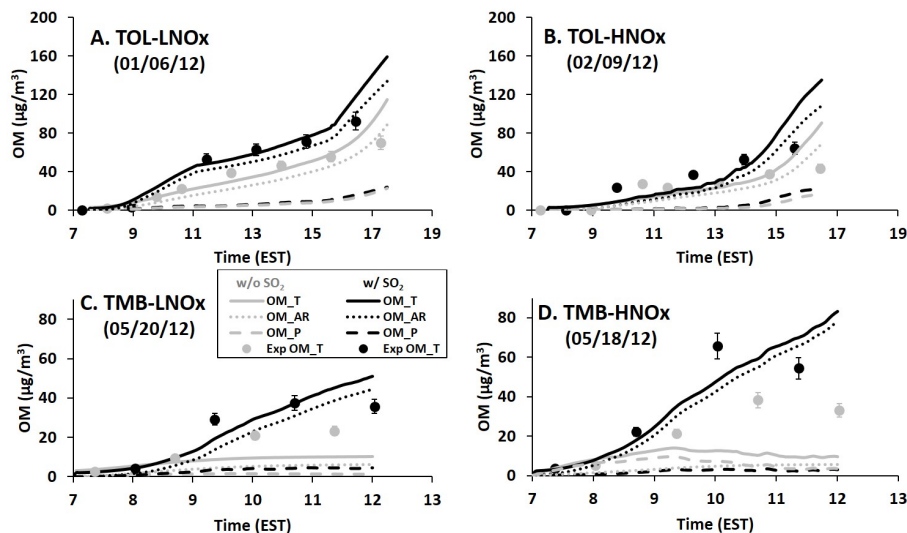


Fig. 3. Time profiles of measured (symbols) and simulated SOA mass concentrations for toluene SOA and 135-TMB SOA under low and high NO_x conditions. The black and gray colors indicate experiments with and without SO_2 , respectively. Solid, dashed, dotted lines represent total OM (OM_T), the OM from partitioning (OM_P), and the OM from the aerosol-phase reaction (OM_{AR}), respectively. The uncertainty associated with OM (about 9%) is estimated from the uncertainties of OC measurements and particle wall loss correction.

Title Page

Abstract

Introduction

Conclusions

References

Tables

Figures

◀

▶

◀

▶

Back

Close

Full Screen / Esc

Printer-friendly Version

Interactive Discussion



A model for aromatic SOA formation by multiphase reactions

Y. Im et al.

Title Page

Abstract

Introduction

Conclusions

References

Tables

Figures

◀

▶

◀

▶

Back

Close

Full Screen / Esc

Printer-friendly Version

Interactive Discussion

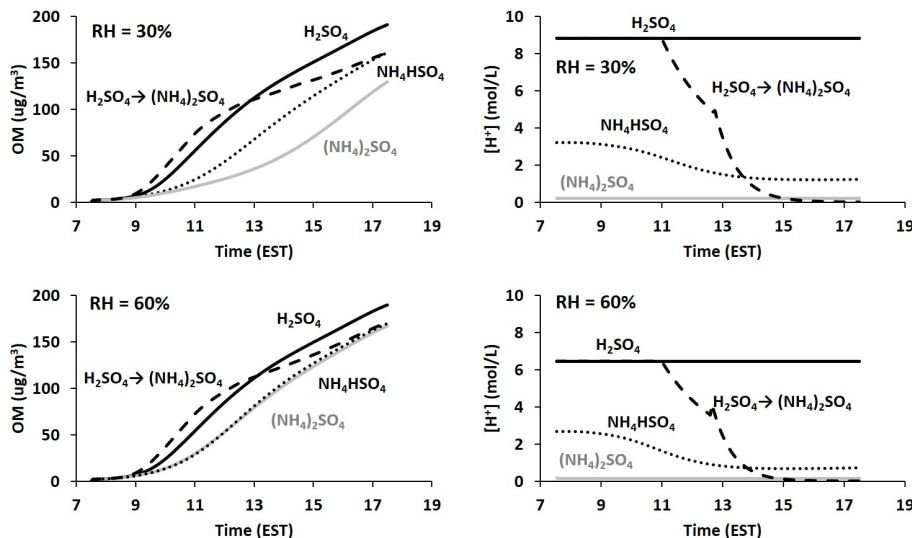


Fig. 4. Time profile of the simulated OM and aerosol acidity ($[\text{H}^+]$, mol L^{-1} in inorganic aerosol) in four different inorganic aerosols: sulfuric acid (black solid line), ammonium bisulfate (black dot), ammonium sulfate (gray solid line), and sulfuric acid with ammonia neutralization (black dash). To mimic atmospheric conditions in the model simulation, inorganic aerosol (e.g. sulfuric acid, ammonium bisulfate, and ammonium sulfate) is added into the chamber at the constant rate ($2.1 \mu\text{g m}^{-3} \text{h}^{-1}$). The total amount of inorganic aerosol introduced into the chamber is $20 \mu\text{g m}^{-3}$. For the case of the neutralization of sulfuric acid with ammonia, sulfuric acid is added for the first 3.5 h (07:30 EST to 11:00 EST), and ammonia is added to the chamber between 11:00 EST to 17:30 EST. For the model simulation, both the sunlight data and the consumption of toluene employ data on Exp 01/06/12 at a constant temperature (298.15 K) at 30% and 60% RH.

A model for aromatic SOA formation by multiphase reactions

Y. Im et al.

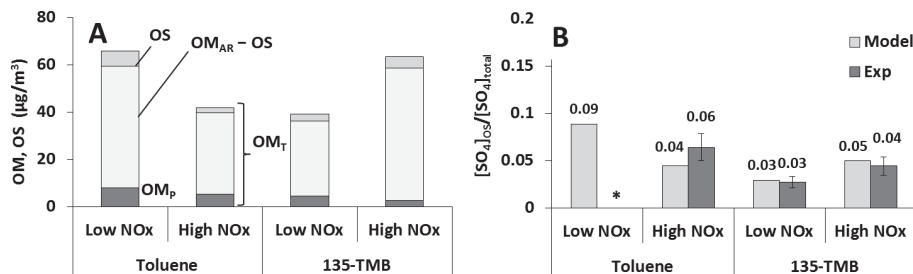


Fig. 5. Model predicted fractions of OM_p, OM_{AR}, and OS of the total SOA for toluene SOA and 135-TMB SOA under two NO_x levels (low and high) (Experiments 1–8 in Table 1) (A). Comparison of the OS fraction of the total sulfate between model prediction and measured using the C-RUV method and PILS-IC (B). The uncertainty associated with the ratio of OS to total sulfate is determined based on uncertainties of C-RUV (about 10 %) and PILS-IC measurements (about 10 %) by the propagation of uncertainty (Ku, 1966). * No experimental data is available.

Title Page

Abstract

Introduction

Conclusions

References

Tables

Figures

◀

▶

◀

▶

Back

Close

Full Screen / Esc

Printer-friendly Version

Interactive Discussion

